International Journal of Future Generation Communication and Networking
Vol. 8, No. 6 (2015), pp. 35-48
http://dx.doi.org/10.14257/ijfgcn.2015.8.6.04

Energy Detector vs. Matched Filtering in 60 GHz Indoor Wireless Communications System

Xiao-Lin Liang[1], Hao Zhang[1,2], Ting-Ting Lv[1] and T. A. Gulliver[2]

[1]*College of Information Science and Engineering, Ocean University of China, Qingdao, 266100, China*
[2]*Department of Electrical and Computer Engineering, University of Victoria, Victoria V8W 3P6, Canada*
xiaolin87liang@163.com, zhanghao@ouc.edu.cn
lvtingting33@163.com, agullive@ece.uvic.ca

Abstract

Whether can the received signal be done with in an even better fashion or not, which is a key factor that can make impact on the accuracy of the ranging and positioning in the 60GHz wireless communication system. There are two mainstream algorithms that may be used for dealing with the signals, which can be segmented into Matched Filtering algorithm and Energy Detection algorithm according to the principle. In order to get the signal processing algorithm that is more suitable for 60GHz millimeter wave. These two algorithms were studied deeply from five aspects respectively such as the distance between nodes, sampling frequency, normalized threshold, the integration period, Signal-to-Noise Ratio. The previous Maximum Energy Selection algorithm and fixed Threshold-Crossing algorithm were compared with the Matched Filtering algorithm in the IEEE 802.15.3c standard indoor channel models. Performance results that are presented verify that it is obvious to improve the accuracy of ranging so long as the received signal is better processed.

Keywords: *60GHz, Matched Filtering, Energy Detector, Maximum Energy Selection, Threshold-Crossing, Signal-to-Noise Ratio*

1. Introduction

As a variety of high-speed applications with rates over Gigabit per second getting into people's production and life, for example High Definition Multimedia Interface(HDML) and Gigabit Wireless Local Area Network(WLAN), the modern production and life demand of high-speed wireless communications services with high quality is becoming stronger and stronger[1-3]. Due to the 7GHz wide spectrums, low-cost Complementary Metal-Oxide-Semiconductor(CMOS) devices implements[4], up to 10W maximum transmit power and other advantages, 60GHz wireless communication technology has received considerable attention which can achieve Gigabits per second(Gbps) level transmission rate.

Multi-Gbps throughput is supported and a very large block of unlicensed spectrum is available worldwide in the 60GHz band. The Federal Communications Commission (FCC) permitted the 60GHz unlicensed effective isotropic radiated power (EIRP) ratio is about 40dBm, which is hundreds or even thousands times than Wireless Fidelity (Wi-Fi), Ultra Wide-band (UWB) and other short-range wireless communication technologies, regulation in China for 44dBm[5]. Even if the 60GHz signal pass through the path loss (PL), the received power is still impressive at the receiving end. The impulse radio communication technologies, which is in the vicinity of the center frequency of 60GHz band, can be more effective to separate the multipath signals at the receiving end because

ISSN: 2233-7857 IJFGCN

of its shorter duration using pulse signal, usually about a hundred picoseconds or less, far less than the multipath propagation delay. The 60GHz mm-wave can achieve higher multipath resolution and realize high precision levels such as centimeters or even millimeters in the process of ranging and location.

The Time of Arrival (TOA) is used here to estimate the distance between two devices in the 60GHz wireless communication system, as it can take full advantage of the higher time resolution available with very short 60GHz pulses. Accurate TOA estimation is the key to precise ranging, but this is very challenging due to the potentially hundreds of multipath components in 60GHz channels. TOA estimation has been extensively studied [6-9].There are two approaches applicable to 60GHz TOA estimation, a Matched Filter (such as a RAKE or correlation receiver) [10-12] or an Energy Detector [13]. In this paper, we focus on that the influence on the accuracy of 60GHz wireless communication system by Matched Filtering and Energy Detector. By comparing the performance of different receiving mode, we try to select the much more suitable way for receiving 60GHz signals in different circumstances.

This paper is organized in the follows manner. In Section II, the 60GHZ wireless communication system in IEEE802.15.3c channel models is introduced. In section III, the existing mainstream algorithm of TOA estimation is discussed briefly. The simulated results and performance comparisons will be shown and discussed in Section IV. Finally, the conclusion will be drawn in Section V.

2. The 60ghz Wireless Communication System In IEEE802.15.3c

Currently two important channel model were developed for 60GHz by the industry as: IEEE 802.15.3c and IEEE 802.11ad. Where the paper used in the simulation was IEEE 802.15.3c standard channel models. The IEEE 802.15.3c channel modeling subgroup provides models for the following frequency ranges and environments: for 60GHz channels covering the frequency range from 57 to 66 GHz, it covers indoor residential, indoor office and library environments (usually with a distinction between Line-Of-Sight (LOS) and Non-Line-Of-Sight (NLOS) properties) [14-18].This paper focus on the indoor residential.

2.1. 60 ghz Pulse Signal

In this article, a Pulse Position Modulation Time-Hopping 60GHz (PPM-TH-60GHz) signal is employed for ranging purposes. The propagation delay (τ) between the transmitter and receiver is estimated for use in the ranging algorithm. The PPM-TH-60GHz signals are very short in time (usually about one hundred picoseconds or less), and can be expressed as

$$s(t) = \sum_{-\infty}^{\infty} p\left(t - jT_s - C_j T_c - a_j \varepsilon\right) \tag{1}$$

Each symbol is represented by a sequence of very short pulses, where T_s is the symbol time. The Time-Hopping (TH) code represented by C is a pseudorandom integer-valued code which is unique for each user (to provide multiple access capability), and T_c is the chip time. ε is the PPM time shift. If a_j is 1, the signal will be shifted in time by ε. If it is 0, there is no time shift. In general, these parameters satisfy the following relationship:

$$(1) C_j T_c + \varepsilon < T_s$$

$$(2) \varepsilon < T_c$$

$$(3)\, a_j \varepsilon < C_j T_c \left(C_j \neq 0 \right)$$

Figure 1 shows the waveform of PPM-TH-60GHz signal waveform $T_c = 1e^{-9}$,

$T_s = 3e^{-9}, C = \{0,2,1,1,1\}$ and $\varepsilon = 0.5e^{-9}$.

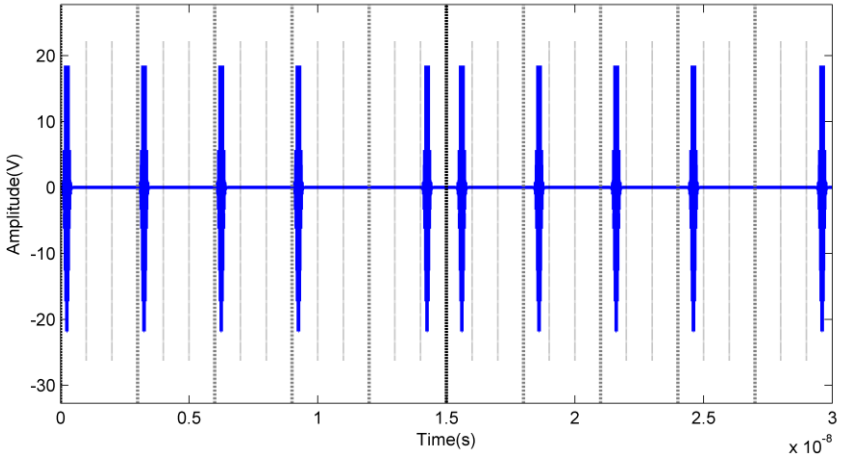

Figure 1. 2PPM-TH-60 GHz Waveform

The 60GHz pulse $p(t)$ is given by, for example, the Gaussian pulse is multiplied by a carrier signal [19]

$$p(t) = \frac{\sqrt{2}}{\alpha} \exp(-2\pi \frac{t^2}{\alpha^2}) \cos(2\pi f_c t) \tag{2}$$

Where α is the shape factor, A smaller shape factor results in a shorter pulse and a larger bandwidth. f_c is the carrier frequency, the value is usually $f_c = 60$ GHz.

2.2. Signal Shift and Path Loss

The path loss is defined as the ratio of the received signal power to the transmit signal power and it is very important for link budget analysis. Unlike narrow-band system, the path loss for a wide-band system such as UWB or mm-wave system, is both distance and frequency dependent. In order to simplify the models, it is assumed that the frequency dependence path loss is negligible and only distance dependence path loss is modeled [20]. The signal path loss, which depends on the propagation distance and the channel (IEEE802.15.3c), is described by

$$PL(d)[dB] = PL_0 + 10 \cdot n \log_{10} \left(\frac{d}{d_0} \right) + X_\sigma [dB]; \; d \geq d_0 \tag{3}$$

Where d_0 and d denote the reference distance, and distance respectively. The path loss exponent n for mm-wave based measurements ranges from 1.2-2.0 for LOS and from 1.97-10 for NLOS, in various different indoor environments. In the presence of wave guiding effects and reverberation effects which lead to increase in power levels by multipath aggregation, *n* can be smaller than 2. X_σ is that the unit dB, with mean zero and variance σ_s for a Gaussian random variable [21]. The Figure 2 shows the PPM-TH-60GHz signal waveform after the path loss. Table 1 summarizes the values of

n, PL_0, σ_s for different environments and scenarios.

Table 1. The PL Exponent, *N* and Standard Deviation for Shadowing

environments	n	PL_0	σ_s
indoor residential(LOS)	1.53	75.1	1.50
indoor residential(NLOS)	2.44	86.0	6.20
indoor office (LOS)	1.16	84.6	5.40
indoor office (NLOS)	3.74	56.1	8.60

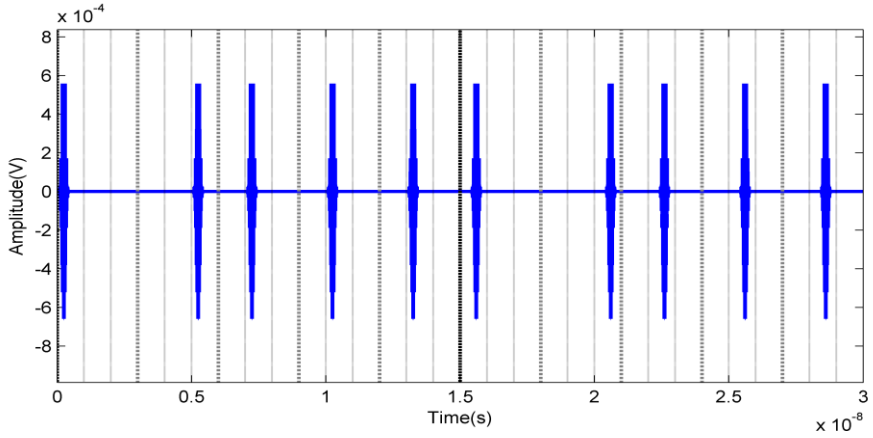

Figure 2. Path Loss

The signal shift can be expressed as:

$$t = dt * floor\left((d / c)/dt\right) \tag{4}$$

Where d denotes the distance between the transmitter and receiver, dt is the sampling period and c is the speed of light which is 299792458m/s in the air. The waveform that moves to the right 10meters (about 0.33 nanoseconds) is showed in the Figure 3.

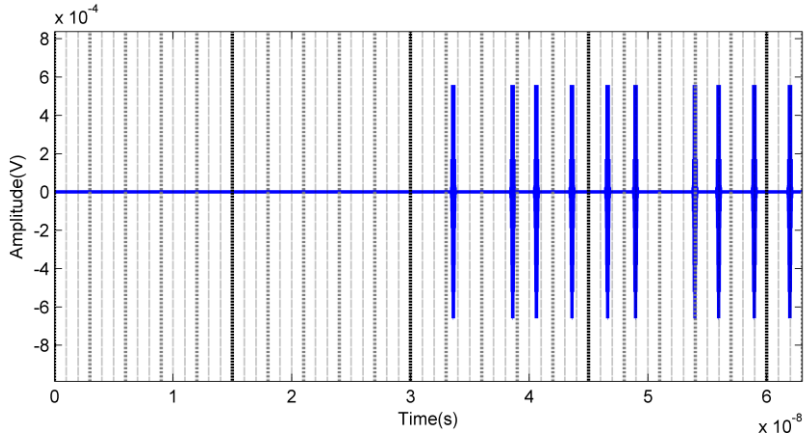

Figure 3. Signal Shift

2.3. Channel Impulse Response in IEEE802.15.3c

Because of the multipath propagation channel, the received signal can be expressed as

$$r(t) = \sum_{i=1}^{L} \beta_i p(t - \tau_i) + n(t) \quad (5)$$

Where L is the number of received multipath components with β_i and τ_i denoting the amplitude and delay of the n^{th} path respectively and $n(t)$ is Additive White Gaussian Noise (AWGN) with zero mean and two-sided power spectral density is $N_0/2$ [14].

In a given channel environment, the received signal can be written again as

$$r(t) = s(t) * h(t) + n(t) \quad (6)$$

Where $s(t)$ is the transmitted signal, and $h(t)$ is the impulse response which can be expressed as:

$$h(t, \theta) = \sum_{k=1}^{K} \sum_{l=1}^{L_K} \mu_{kl} \delta(t - T_k - \tau_{kl}) \delta(\theta - \theta_k - \omega_{kl}) \quad (7)$$

Where $\delta(.)$ is the dirac delta function, K is the total number of clusters and L_k is total number of rays in k^{th} cluster. The scalars μ_{kl}, τ_{kl} and ω_{kl} denote the complex amplitude, delay and azimuth of the k^{th} ray of the l^{th} cluster. Similarly, the scalars T_k and θ_k represent the delay and mean angle-of-arrival (AOA) of the k^{th} cluster. The Figure 4 denote the signal $s(t) * h(t)$.

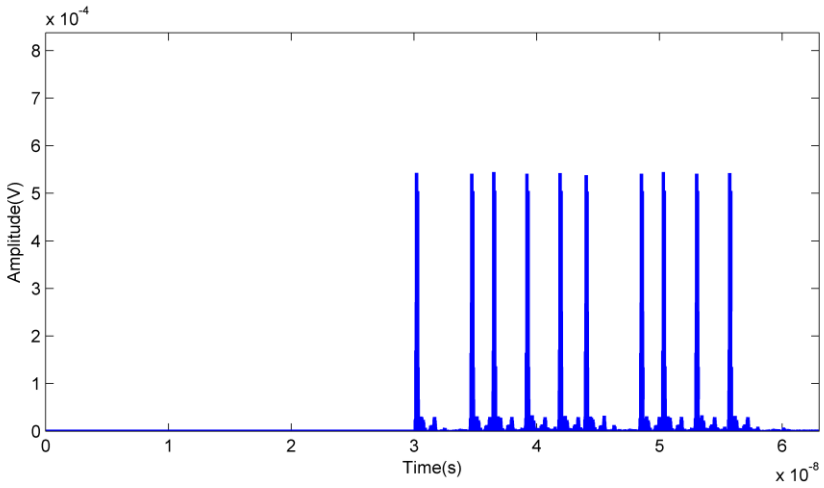

Figure 4. Signal with Impulse Response

2.4. Additive White Gaussian Noise

Additive White Gaussian Noise (AWGN) is the traditional noise with mean is zero and two-sided power spectral density is $N_0/2$. The Figure 5 denote the received signal with AWGN.

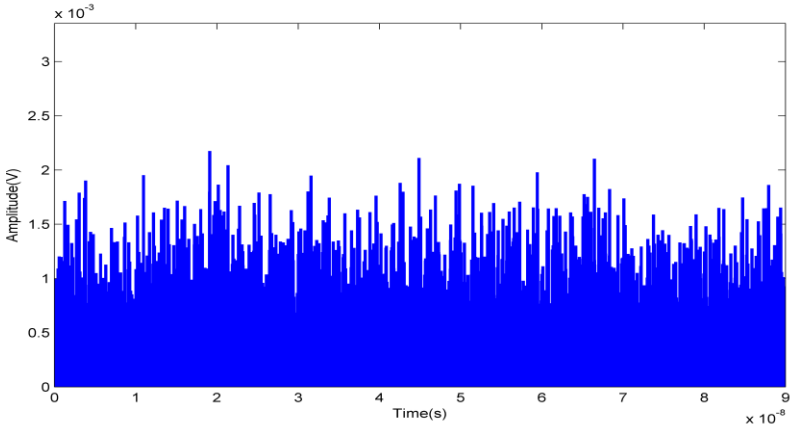

Figure 5. Received Signal with AWGN

3. TOA Estimation

3.1. TOA Estimation Based on Matched Filtering

Matched Filtering is one of the optimal filters. The output value reaches the maximum when the input signal having a particular waveform. It is generally considered the Matched Filtering is the correlation calculation. The correlation function can be expressed as:

$$r_{xs}(\tau_d) = \frac{1}{T_0}\int_{T_0} r(t)\,s(t-\tau_d)\,dt \tag{8}$$

Where $T_0 = T_p/2$ is integration cycle, T_p is pulse width, $r(t)$ is the received signal, and $s(t)$ is the transmitting signal. The goal is to obtain an unbiased estimate of the TOA τ by observing the received signal $r(t)$. A correlator receiver is used to correlate $r(t)$ with a reference template $r(t-\tau)$ (the output of correlate is shown in the Figure6 and calculates the propagation delay τ corresponding to the position of the correlation peak given by

$$\hat{\tau} = \arg\max_{\tau} \int r(t)\,s(t-\tau)\,dt \tag{9}$$

The distance between the transmitter and receiver can then be estimated as $d = c \times \tau$, where *c* is the speed of light.

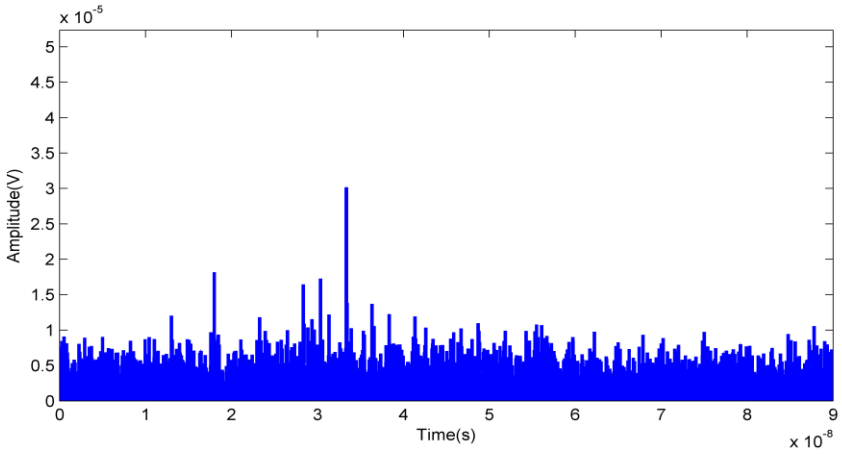

Figure 6. Output with Matched Filtering in Channel CM1.1

3.2. TOA Estimation Based on Energy Detector

As shown in Figure 7 [22-23], after the amplifier, the received signals are squared, and then input to an integrator with integration period T_b. Because of the inter-frame leakage due to multipath signals, the integration duration is $3T_f / 2$, so the number of signal values for Energy Detector is $Nb = 3T_f / 2T_b$. The integrator outputs can be expressed as:

$$z[n] = \sum_{i=1}^{N} \int_{(i-1)T_f + (c_j + n - 1)T_b}^{(i-1)T_f + (c_j + n)T_b} r^2(t)dt \tag{10}$$

Where $n \in \{1, 2, .., Nb\}$ denotes the sample index with respect to the starting point of the integration period and N is the number of pulses per symbol. The final output of integrator is shown in the Figure 8.

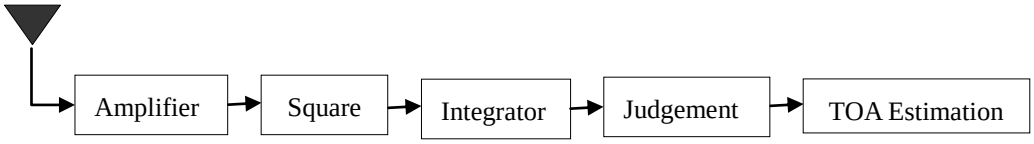

Figure 7. Block Diagram of Energy Detection Receiver

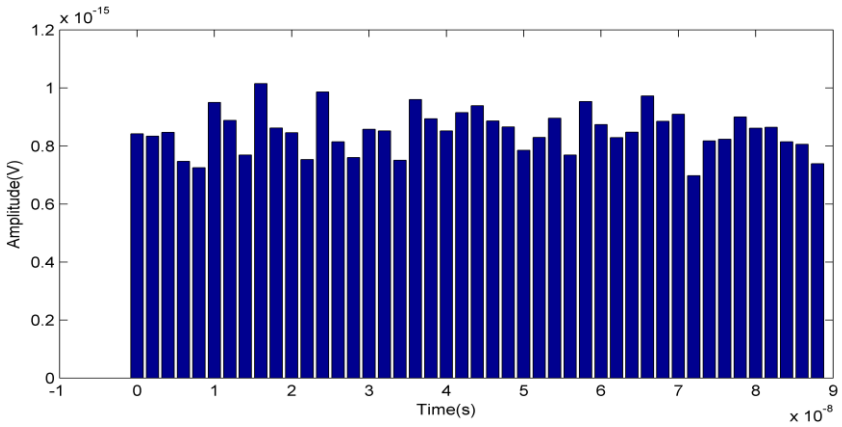

Figure 8. Output with ED in Channel CM1.1

There are many TOA estimation algorithms based on energy detection for determining

the start of a received signal. The simplest is Maximum Energy Selection, which chooses the maximum energy value to be the first. The TOA is estimated as the center of the corresponding integration period appropriate threshold. In this case, the TOA estimate is given by

$$\tau_{MES} = \left\lfloor \arg\max_{1 \le n \le N_b} \{ z[n] \} - 0.5 \right\rfloor Tb \tag{11}$$

It is difficult to determine an appropriate threshold directly, so usually a normalized threshold α is calculated. Using α , ξ is given by

$$\xi = \alpha \left(\max(z(n)) - \min(z(n)) \right) + \min(z(n)) \tag{12}$$

The TOA estimate, τ_{TC} , is then obtained using (13).

$$\tau_{TC} = \left\lceil \arg\min_{1 \le n \le n_{\max}} \{ n \mid z[n] \ge \xi \} - 0.5 \right\rceil Tb \tag{13}$$

4. Simulation Results and Performance Comparisons

In order to fully study the effects on performance of 60GHz wireless communication system in different receiving way, the CM1 (residential LOS) and the CM2 (residential NLOS) channel models from the IEEE802.15.3c standard is employed respectively. We made great amount of simulations, for each simulation, 1000 channel realizations were generated at the same time. The emphasis of the study that we made focused on the following aspects:

(1)What is the relationship between the distance from the transmitter to the receiver and receiving method;

(2)How can the accuracy of the ranging be influenced because of change of the signal sampling frequency in various of receiving method;

(3)Whether the signal-to-noise ratio (SNR) will affect the results of ranging or not;

(4)What influence may be exerted on the accuracy of the ranging as a result of different normalized threshold α ;

(5)What impact may be made on the accuracy of the ranging as a result of different integration period T_b ;

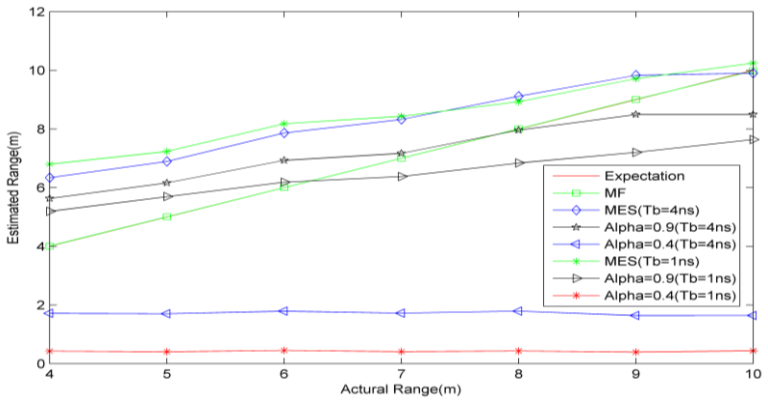

Figure 9. Ranging with Distance in Channel CM1.1

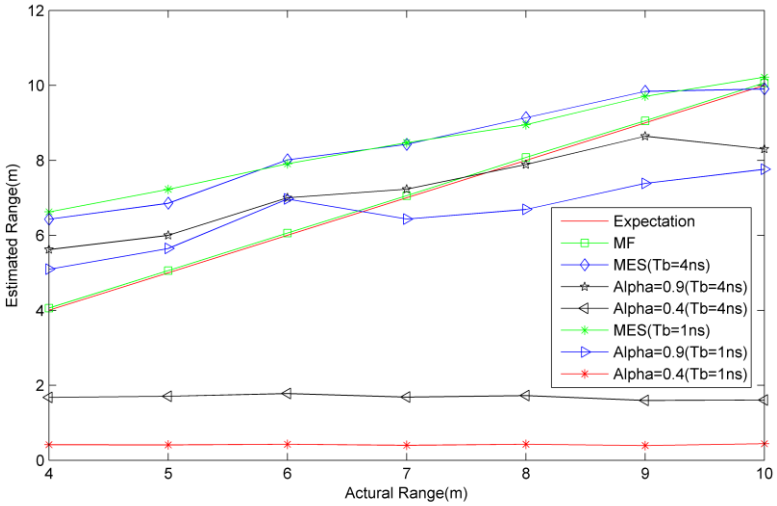

Figure 10. Ranging with Distance in Channel CM2.1

Aimed at the first problem, 1000 channel realizations were generated and sampled at $f = 10^{11}$ Hz and SNR=5dB for different receiving methods. The distance ranges from 4 to 10 meters. As shown in Figure 9 and Figure 10. Whether in LOS or NLOS environment, ranging results based on Matched Filtering performed much better relative to other methods. The ranging accuracy under LOS is significantly higher than that in NLOS environment. For Maximum Energy Selection algorithm, ranging error will gradually smaller with the increase of the distance between nodes, integration period has little effect on the range accuracy.

For the threshold-crossing algorithm, in the case of the same Integration Period, ranging error will degrade with the Normalized Threshold increases, at the same time, the Normalized Threshold should be increased correspondingly in order to improve the range accuracy with the increase of the distance vice versa. (For example, in the range of 7m-10m, the accuracy of rang is significantly higher when Integration Period equal to 4ns than the Integration Period equal to 1ns).

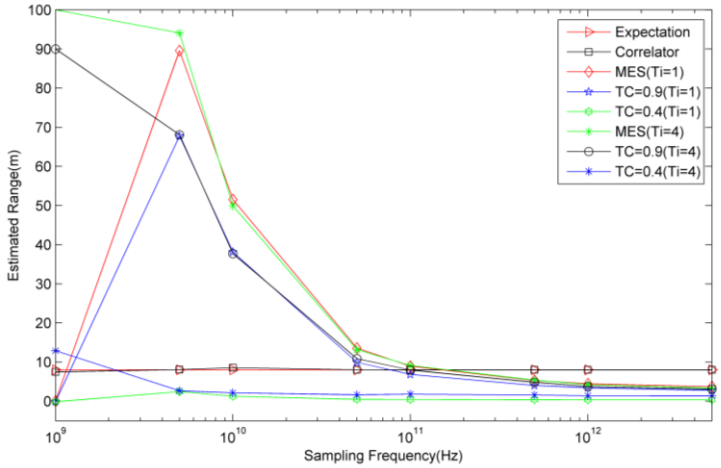

Figure 11. Ranging with Frequency in Channel CM1.1

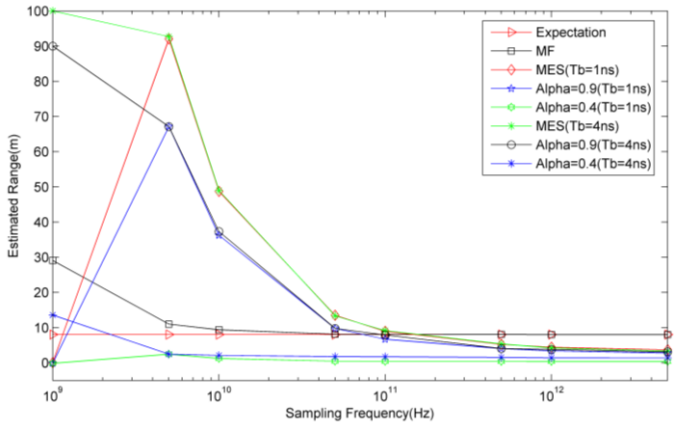

Figure 12. Ranging with Frequency in Channel CM 2.1

As for the relationship between the accuracy of range and Sampling Frequency, 1000 channel realizations were generated and sampled at SNR=5dB for different receiving methods. The Sampling Frequency ranges from 0.1GHz to 1000GHz. Under different channel environment, the final results of the simulation what influence may be exerted on the accuracy of the ranging as a result of different Sampling Frequency are displayed in the Figure 11 and Figure12.

In theory, with the increase of the Sampling Frequency, the ranging accuracy should gradually improve, but in the real environment, because of the influence of various factors such as noise and characteristics of 60GHz pulse signal, that is not the case. As can be seen from the simulation results, Whether in LOS or NLOS environment, for the Matched Filtering algorithm, when Sampling Frequency reaches a certain value (*e.g.*, when $f = 10^{11}$ Hz), the accuracy will not significantly be improved with the increase of the Sampling Frequency. At the same time, the time it takes the Matched Filtering algorithm will be significantly prolonged.

In particular, when the sampling frequency is too high (*e.g.*, when $f = 10^{12}$ Hz), the time it takes will be dozens of times even hundreds times longer than the Energy Detector algorithm. Therefore, it is not realistic to improve accuracy by increasing the signal Sampling Frequency due to the limitation of hardware, materials technology and so on in reality. In connection with the problem, the Energy Detector algorithm has incomparable advantages in term of saving time. For the Energy Detector algorithm, overall, the error increases with the increasing of the Sampling Frequency, and then decreases. For the Threshold Crossing algorithm, the Integration Period should decrease when the Sampling Frequency is low vice versa.

For different Sampling Frequency, the Normalized Threshold has little influence on ranging precision. Although it can be appropriate to reduce the Sampling Frequency for the Energy Detector algorithm, but it must meet $Tb \geq (1/f)$. (*e.g.*, when $Tb = 1$ ns and $f = 10^{8}$ Hz, the Energy Detector algorithm is invalid). There is no such restriction in terms of the Matched Filtering algorithm. Although the error increases rapidly when the Sampling Frequency is too petty, but it still exists. (*e.g.*, when $f = 10^{8}$ Hz, the estimation is13.2m in the CM1 (residential LOS) but 186.0722m in the CM2 (residential NLOS) channel models.)

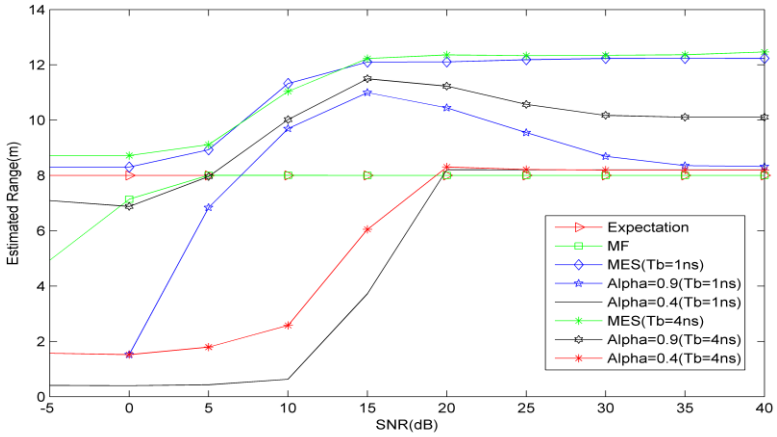

Figure 13. Ranging with SNR in Channel CM 1.1

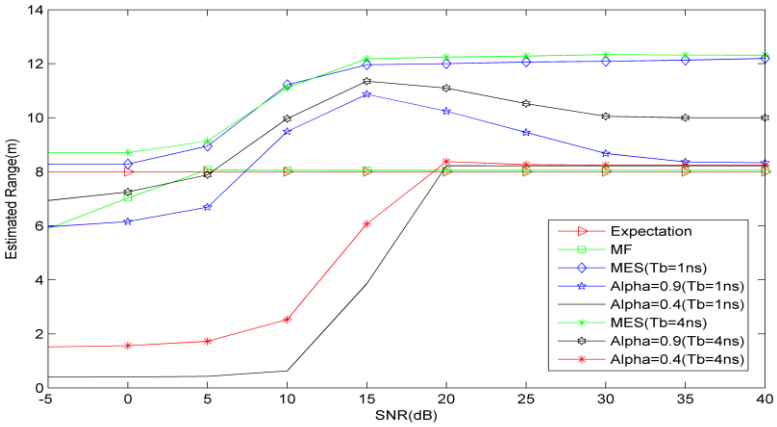

Figure 14. Ranging with SNR in Channel CM2.1

As for the third problem, 1000 channel realizations were generated and sampled at $f = 10^{11}$ Hz for different receiving methods. The SNR ranges from -5dB to 40dB. Under different channel environment, the final results of the simulation whether the SNR will affect the results of ranging or not as a result of different SNR are displayed in the Figure 13 and Figure 14.

In theory, with the increase of the SNR, the ranging accuracy should gradually improve, but in the real environment, because of the influence of various factors such as noise and characteristics of 60GHz pulse signal, that is not the case. As can be seen from the simulation results, whether in LOS or NLOS environment, for the Matched Filtering algorithm, when SNR reaches a certain value (*e.g.*, when SNR=20dB), the accuracy will not significantly be improved with the increase of the SNR, but at the same time, when the SNR decreased less than 5dB, the range error will increase significantly.

For the Maximum Energy Selection and Threshold Crossing (when Normalized Threshold is 0.9) algorithm, overall, the error increases with the increasing of the SNR, and then decreases. But the accuracy of ranging stays almost level when the SNR less than 5dB. For Threshold Crossing (when Normalized Threshold is 0.4) algorithm, the error decreases rapidly with the increasing of the SNR, and then flats.

5.Conclusion

In this paper, in order to process the received signals much more accurately, two algorithms (such as the Matched Filtering algorithm and the Energy Detectoring algorithm) were studied deeply from five aspects respectively such as the distance between nodes, sampling frequency, normalized threshold, the integration period, signal-to-noise ratio under different channel environments. We can see from the simulated results. No matter under what circumstances, the Matched Filtering algorithm performance much more superior than the Energy Detector algorithm. But in practice, the Matched Filtering algorithm is not easy to achieve, which is limited by many objective conditions (such as hardware, material technology, *etc*.). At the same time, although the Energy Detector algorithm is slightly inferior in performance compared with the Matched Filtering algorithm, it is much more practical associated with lower hardware requirements.

A Matched Filtering is the optimal strategy for TOA estimation, where a correlator template is matched exactly to the received signal. However, a receiver operating at the Nyquist sampling rate makes it very difficult to align with the multipath components of the received signal. In addition, a Matched Filtering requires a priori estimation of the channel, including the timing, fading coefficient, and pulse shape for each component of the impulse response. Because of the higher sampling rates and channel estimation, a Matched Filtering may not be practical in many applications. As opposed to a more complex Matched Filtering, an Energy Detector is a non-coherent approach to TOA estimation. It consists of a square-law device, followed by an integrator, sampler and a decision mechanism. The TOA estimate is made by comparing the integrator output with a threshold and choosing the first sample to exceed the threshold. This is a convenient strategy that directly yields an estimate of the start of the received signal. Thus, a low complexity, low sampling rate receiver can be employed without the need for a priori channel estimation. So in the future, we will try to design the fixed threshold for the Energy Detector.

Acknowledgments

The authors would like to thank colleagues from College of Information Science and Engineering, Ocean University of China for measurement support, and Department of Electrical and Computer Engineering, University of Victoria for valuable supports and discussions. This work is supported by the Nature Science Foundation of China under grant No.60902005 and Qingdao International Science and Technology Cooperation Projects of Qingdao no. 12-1-4-137-hz.

References

[1] S.K. Yong and C.C. Chong, “An Overview of Multigigabit Wireless through Millimeter Wave Technology: Potentials and Technical Challenges”, EURASIP Journal on Wireless Communications and Networking, vol. 2007, **(2007)**, pp. 1-10.
[2] R.C. Daniels and R.W. Heath, “60 GHz wireless communications: emerging requirements and design recommendations”, IEEE Vehicular Technology Society, vol. 3, **(2007)**, pp. 41-50.
[3] C.C. Chong, F.M. Peter and Smulders, “60GHz-Millimeter-Wave Radio Principle, Technology, and News Results”, EURASIP Journal on Wireless Communications and Networking, vol. 2007, **(2007)**, pp. 1-8.
[4] L. Zhang, C.Y. Zhou and H.R. Wang, “A fully integrated 60GHz four channel CMOS receiver with 7GHz ultra-wide band width for IEEE 802.11ad standard”, Communication, China, vol. 11, **(2014)**, pp. 42-50.
[5] S.K. Yong, P.F. Xia and V.G. Alberto, “60GHz Technology for Gbps WLAN and WPAN: From Theory to Practice”, Press of China Machine, Beijing, **(2013)**.
[6] D. Dardari, A. Conti, U. Ferner, A. Giorgetti and M. Z. Win, “Ranging with ultra-wide bandwidth signals in multipath environments,” Proceedings of IEEE, vol. 97, **(2009)**, pp. 404-426.

[7] D. Dardari, A. Giorgetti and M.Z. Win, "Time-of-arrival estimation of UWB signals in the presence of narrowband and wideband interference", Proceedings of IEEE International Conference On Ultra-Wideband, Singapore, **(2007)**.
[8] A. Abbasi and M.H. Kahaei, "Improving source localization in LOS and NLOS multipath environments for UWB signals", Proceedings of 14th International CSI Computer Conference, Tehran, **(2009)**.
[9] A.Y.Z. Xu, E.K.S. Au, A.K.S. Wong and Q. Wang, "A novel threshold-based coherent TOA estimation for IR-UWB systems", IEEE Transactions on Vehicular Technology, vol. 58, **(2009)**, pp. 4675-4681.
[10] M.E. Sahin, I. Guvenc and H. Arslan, "Optimization of energy detector receivers for UWB systems", 61st IEEE Vehicular Technology Conference, vol. 2, **(2005)**, pp.1386-1390.
[11] I. Guvenc, Z. Sahinoglu and P. V. Orlik, "TOA estimation for IR-UWB systems with different transceiver types", IEEE Transactions on Microwave Theory and Techniques, vol. 54, **(2006)**, pp. 1876-1886.
[12] S.H. Wu and N.T. Zhang, "A Two-Step TOA Estimation Method for UWB Based Wireless Sensor Networks", Journal of Software, vol. 18, **(2007)**, pp. 1164-1172.
[13] L.J. Ge, L.Zhu and X.F. Yuan, "Understanding Ultra Wide Band Radio Fundamentals", Publishing House of Electronics Industry, Beijing, **(2005)**.
[14] C.R. Andersonn and T.S. Rappaport, "In-building wideband partition loss measurements at 2.5 and 60GHz," IEEE Transactions on Wireless Communications, vol. 3, **(2004),** pp. 922-928.
[15] S. Collong, G. Zaharia and G. E. Zein, "Influence of the human activity on wide-band characteristics of the 60GHz indoor radio channel", IEEE Transactions on Wireless Communications, vol. 3, **(2005),** pp. 2396-2406.
[16] A. Maltsev, R. Maslennikov and A. Sevastyanov, "Experimental investigations of 60GHz WLAN systems in office environment", IEEE Journal on Selected Areas in Communications, vol. 27, **(2009)**, pp.1488-1499.
[17] M.G. Sanchez, A.V. Alejos and I. Cuinas, "Comparision of space deversity performance in indoor radio channels at 40GHz and 60GHz", Proceedings of European Conference on Wireless Technology, EuWiT, , **(2008)**.
[18] H.B. Yang, F.M. Peter and Smuiders, "Channel characteristics and transmission performance for various channel configurations at 60GHz", EURASIP Journal on Wireless Communicatins and Networking, vol. 1, **(2007)**, pp. 43-43.
[19] N. Li, "Study on the properties of 60 GHz impulse radio communication system", Ocean University of China, Qingdao, **(2012)**.
[20] P.F.M. Smulder, "Statistical Characterzation of 60GHz Indoor Radio Channels". IEEE Transactions on Antennas and Propagation, vol. 57, **(2009)**, pp. 2820-2829.
[21] S.K. Yong, "IEEE 802.15.3c Channel Modeling Sub-committee Report". IEEE 15-07-0584-01-003c. Orlando, USA, **(2007)**.
[22] S.H. Wu, Q.Y. Zhang and N.T. Zhang, "A UWB Ranging Method Based on Weighted Energy Detection", Journal of Electronics and Information Technology, vol. 31, **(2009)**, pp. 1946-1951.
[23] X. R. Cui, C. L. Wu and J. Li, "UWB energy detection based localization algorithm simulation", Microcomputer Applications, vol. 27, **(2011)**, pp. 20-22.

Authors

Xiao-Lin Liang now studies in College of Information Science and Engineering and is a Master candidate in Ocean University of China. His research interests include ultra-wideband radio systems, 60GHz wireless communication system.

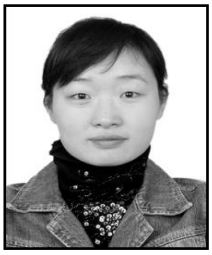

Ting-Ting Lv received the Ph. D. degree in College of Information Science and Engineering from Ocean University of China in 2013. She is now a lecture in College of Information Science and Engineering. Her research interests include ultra-wideband radio systems, 60GHz wireless communication system.

Hao Zhang received the MBA degree in New York Institute of Technology, American in 2001 and the Ph. D. degree in Electrical and Computer Engineering from the University of Victoria, Canada in 2004. He was a Project Manager for Microsoft Inc. in United States during January 2000-May 2000. During 2004-2008, he was the Vice President for the United States Gamma Capital Inc. He is now an Adjunct Assistant Professor in the Department of Electrical and Computer Engineering. Also he becomes a professor and the Ph. D. supervisor in College of Information Science and Engineering from Ocean University of China in 2006. His research concerns ultra-wideband radio systems, 60GHz wireless communication system and MIMO wireless communication.

T. Aaron. Gulliver received the Ph. D. degree in Electrical and Computer Engineering from the University of Victoria, Canada in 1989. He is now a professor and the Ph. D. supervisor in the Department of Electrical and Computer Engineering. In 2002, he becomes a Fellow of the Engineering Institute of Canada, and in 2012 a Fellow of the Canadian Academy of Engineering. He is also a senior member of IEEE. His research concerns information theory and communication theory, algebraic coding theory, crytography and smart grid and ultra wideband communication.